

AD-A263 212



(2)

PL-TR-92-2266

DISCHARGE OF ELECTRICALLY CHARGED CLOUDS

**Jean-Claude Diels
Xin Miao Zhao
Chao Yung Yeh
Cai Yi Wang**

**University of New Mexico
Department of Physics and Astronomy
Albuquerque, NM 87131**

26 October 1992



**Final Report
September 1990 - September 1992**

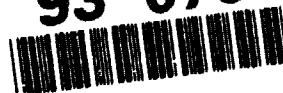
Approved for public release; distribution unlimited



**PHILLIPS LABORATORY
Directorate of Geophysics
AIR FORCE MATERIEL COMMAND
HANSCOM AIR FORCE BASE, MA 01731-5000**

93 4 09 08 7

256 690
93-07517
29P8



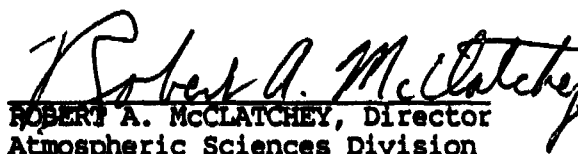
"This technical report has been reviewed and is approved for publication"



ROBERT O. BERTHEL
Contract Manager



DONALD D. GRANTHAM, Chief
Atmospheric Structure Branch



ROBERT A. MCCLATCHEY, Director
Atmospheric Sciences Division

This report has been reviewed by the ESC Public Affairs Office (PA) and is releasable to the National Technical Information Service (NTIS).

Qualified requesters may obtain additional copies from the Defense Technical Information Center. All others should apply to the National Technical Information Service.

If your address has changed, or if you wish to be removed from the mailing list, or if the addressee is no longer employed by your organization, please notify PL/IMA, Hanscom AFB, MA 01731-5000. This will assist us in maintaining a current mailing list.

Do not return copies of this report unless contractual obligations or notices on a specific document requires that it be returned.

REPORT DOCUMENTATION PAGE			Form Approved OMB No 0704-0188	
<small>Public reporting burden for this collection of information is estimated to average 1 hour per response, including the time for reviewing instructions, searching existing data sources, gathering and maintaining the data needed, and completing and reviewing the collection of information. Send comments regarding this burden estimate or any other aspect of this collection of information, including suggestions for reducing this burden, to Washington Headquarters Services, Directorate for Information Operations and Reports, 1215 Jefferson Davis Highway, Suite 1204, Arlington, VA 22202-4302, and to the Office of Management and Budget, Paperwork Reduction Project (0704-0188), Washington, DC 20503.</small>				
1. AGENCY USE ONLY (Leave blank)		2. REPORT DATE 26 October 1992	3. REPORT TYPE AND DATES COVERED Final Report, Sept 1990-Sept 1992	
4. TITLE AND SUBTITLE Discharge of Electrically Charged Clouds			5. FUNDING NUMBERS PE 62101F PR ILIR TA OB WU AA Contract F19628-90-K-0050	
6. AUTHOR(S) Jean-Claude Diels, Xin Miao Zhao, Chao-yuen Yeh and Cai Yi Wang				
7. PERFORMING ORGANIZATION NAME(S) AND ADDRESS(ES) Department of Physics and Astronomy University of New Mexico Albuquerque, NM 87131			8. PERFORMING ORGANIZATION REPORT NUMBER	
9. SPONSORING/MONITORING AGENCY NAME(S) AND ADDRESS(ES) Phillips Laboratory Hanscom AFB, MA 01731-5000 Contract Manager: Arnold Barnes/GPAA			10. SPONSORING/MONITORING AGENCY REPORT NUMBER PL-TR-92-2266	
11. SUPPLEMENTARY NOTES				
12a. DISTRIBUTION/AVAILABILITY STATEMENT Approved for public release; distribution unlimited			12b. DISTRIBUTION CODE	
13. ABSTRACT (Maximum 200 words) <p>In a one year program, we have established a new mechanism for triggering lightning using low energy (less than 1 mJ) ultrashort (subpicosecond) pulses. A pre-ionized "needle-shaped" path is created by three to four photon ionization of oxygen or applied field results in a local enhancement of the field, sufficient to reach avalanche breakdown. Measurement of multiphoton ionization cross section have established that a few mJ/cm² in 200 fs at 248nm are sufficient to create 10¹³ electrons per cm³. Laser induced discharge of 90 KV over 25cm have been demonstrated with ns pulses at 248nm, at pressure of 1/7 atm.</p> <p>This result and the theory indicate that less than 1 mJ in less than 1 ps duration pulses at 248nm should induce the discharge at atmospheric pressure. A fs laser oscillator-amplifier has been assembled to perform such tests.</p>				
14. SUBJECT TERMS Lightning Laser Triggered Lightning			15. NUMBER OF PAGES 30	
			16. PRICE CODE	
17. SECURITY CLASSIFICATION OF REPORT Unclassified	18. SECURITY CLASSIFICATION OF THIS PAGE Unclassified	19. SECURITY CLASSIFICATION OF ABSTRACT Unclassified	20. LIMITATION OF ABSTRACT SAR	

Contents

1 Objective	1
2 Motivation	1
3 Background	1
4 Highlights of the method	2
5 Theory	2
5.1 Fs pulse propagation and compression	3
5.2 Evolution towards a streamer	6
6 Experimental work	7
6.1 The oscillator	8
6.2 YAG laser Amplifier	8
6.3 Frequency tripling assembly	10
6.4 KrF laser UV (248nm) pulse amplifier	11
6.5 Synchronizer	12
6.6 Pulse measurement without nonlinear process	13
6.7 Ionization cross sections	14
6.8 High Voltage Cell	15
6.9 Inducing 100 kV discharge in air	17
7 Conclusion	19
Reference	20
A Pulse propagation/compression	22
B Evolution towards a streamer	23

DTIC QUALITY INSPECTED 4

Accession For	
NTIS GRA&I	<input checked="" type="checkbox"/>
DTIC TAB	<input type="checkbox"/>
Unannounced	<input type="checkbox"/>
Justification	
By _____	
Distribution/	
Availability Codes	
Dist	Avail and/or Special
A-1	

1 Objective

To develop a safe and reliable method to discharge thunderclouds. The target field at which we aim to trigger the lightning is $1/10$ of the self breakdown field in air.

2 Motivation

The ability to continuously discharge thunderclouds over rocket launch pads and airports would prevent the delays and hazards associated with lightning. Lightning strikes have damaged the radar cone of aircrafts, and destroyed rockets [1] through the electromagnetic pulse affecting the navigational computer. This development will also have an impact on storm research. A sudden change in the electromagnetic forces present in a cumulonimbus may affect its development. It has been thought in the past that a shock wave such as caused by thunder at an early stage of a storm development may cause rain, **preventing hail** [2] that would occur at a later stage. The ability to trigger lightning in and to the cloud would lead to a better modeling and understanding of the storms, and even the prospect of having a limited action on them.

3 Background

A commonly used method to trigger lightning is to fire a rocket trailed by a grounding wire [3, 4] through the 100 m height space charge layer shielding the ground. As compared to the method proposed here, this method has the following disadvantages:

- The space charges accumulate around the rocket fast enough to shield it. Obviously, this could not occur with a conductive volume created at the speed of light.
- While there is a *preferential* path created for the lightning, there is not the ten-fold field enhancement that is required to ensure that no other element (airplane, rocket can trigger the lightning).

- The rockets cannot be launched on a continuous bases. The repetition rate of the laser trigger can easily exceed 10 Hz.

Another method that has been considered in the past and is still being investigated by a Japanese group [5] is lightning triggering with a powerful CO_2 laser. The main disadvantage of the latter method is that it requires a laser field exceeding the avalanche breakdown field. The laser produced plasma is thus opaque to the radiation, a fact that limits the range over which an ionized path can be created.

4 Highlights of the method

Charge seeding A pencil shaped volume of free electrons is created by 3- and 4- photon ionization of oxygen and nitrogen in a region of high field, using a fs pulse at 248 nm.

Pulse propagation The fs pulse is given a negative frequency sweep (downchirp) such that pulse compression in air occurs. The resulting peak amplification compensates the depletion due to multiphoton ionization, and linear absorption.

Photodetachment A long pulse of visible light (530 nm) is launched simultaneously, to maintain the conductive path (by photodetaching the O^- and O_2^- ions).

Field enhancement The motion of the charges in the external field is such that an internal field is created, with a ten fold local enhancement at the "tip" of the pencil. When the enhanced local field reaches the threshold for avalanche breakdown, the discharge is initiated.

5 Theory

We have established a theoretical model for the fs triggering of lightning, and performed numerical calculations. The theoretical work detailed in the following subsections include:

- Calculation of pulse propagation, compression and multiphoton ionization
- Prediction of conditions of chirp and focusing that lead to optimum uniform "seeding" of electrons
- Calculation of the charge evolution and resulting field enhancement
- Prediction of the optimum ratio of diameter to height for the ionized column.

5.1 Fs pulse propagation and compression

The procedure for calculating the pulse propagation and compression is outlined in Appendix A and in ref. [6, 7] We will present here only a brief summary of the main results.

Fig. 1 shows the ionized volume created by focusing the beam to a 1 mm beam waist at 50 m from ground. A fairly localized and narrow pencil of charges is created, with a density in excess of $2 \times 10^{13} \text{ cm}^{-3}$ when a downchirped Gaussian beam is used. For larger pulse energies, the ionization volume is ahead of the beam waist, as illustrated in Fig. 2. It may be advantageous to focus the beam at higher altitudes, use much higher pulse energies, in order to create a ionization volume of larger diameter. There is a compromise to be reached:

- For a given pulse energy, the density of photoelectrons increases proportionally to $1/w^6$ (oxygen) or $1/w^8$ (nitrogen), where w is the transverse dimension of the beam
- For a cylinder of radius r ionized at 10^{13} cm^{-3} , the local enhancement of the field is fastest for $r \geq 5 \text{ cm}$

The second condition results from the computer simulations of the evolution of the charges under the applied field presented in the following section. The optimum diameter of the ionization volume will have to be determined experimentally, as it is a function of the size of the fs laser source available for triggering the lightning. Another important consideration is the location (altitude) of the peak field. Our calculations as well as the preliminary discharge tests show that it is preferable to locate the ionized volume in the

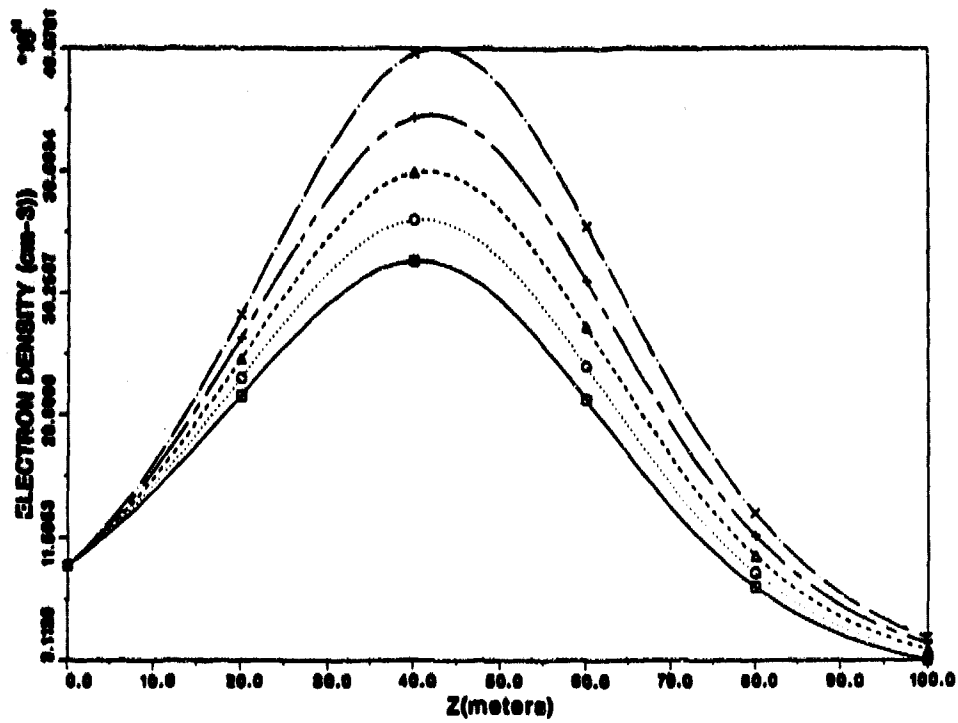


Figure 1:
Electron density versus distance (height above ground) for a 200 fs full width half maximum (FWHM) Gaussian beam of 5 mJ energy focused to a beam waist of $w_0 = 1\text{ mm}$ at 50 m. The pulse temporal shape is $\mathcal{E}(t) = \mathcal{E}_0 \exp\left\{-(1 + i\frac{c}{2})\left(\frac{t}{\tau_g}\right)^2\right\}$ with values for the chirp coefficient $c = 0, 0.5, 1.0, 1.5$, and 2 , corresponding to solid, dotted, dashed, long-dash and dash-dotted lines, and $\tau_g = 200 \text{ fs}/\sqrt{2 \ln 2}$.

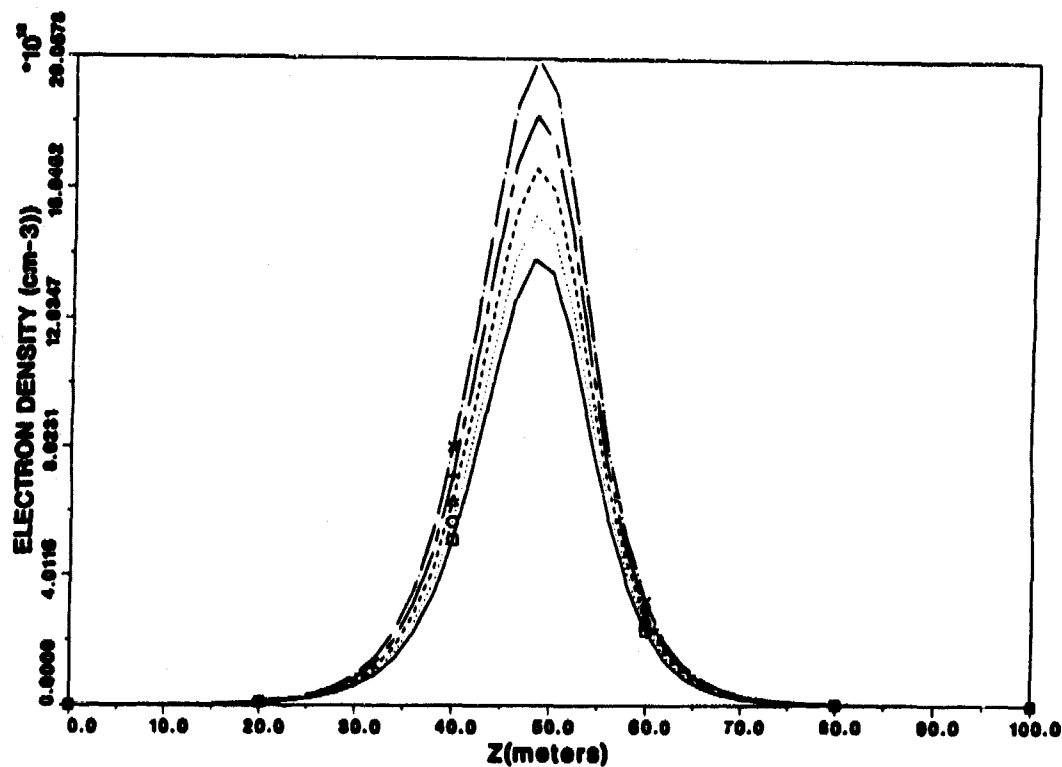


Figure 2:

Electron density versus height, for a 10 mJ 200 fs (FWHM) Gaussian beam focused to a waist of $w_0 = 2$ mm at 50 m. The pulse shape is the same as in Fig. 1 with the chirp coefficients 0, 0.5, 1, 1.5 and 2 corresponding to solid, dotted, dashed, long-dash and dash-dotted lines.

region of highest field. Near the earth, the fields do not generally exceed 50 kV/m [8], while fields as high as 3 MV/m have been measured at high altitude.

5.2 Evolution towards a streamer

This subsection summarizes our theoretical results, which are outlined in more details in Appendix B and in refs. [7, 9, 10].

The purpose of the theory is to determine whether the charge seeding produced by fs photoionization will lead to the formation of a streamer, and trigger the lightning.

We approximate the results of the preceeding section by a cylinder of radius r containing a Gaussian distribution of electrons $N_e(z)$ and ions $N_i(z)$. Under influence of the external field, the electrons and ions will separate, creating a local field that opposes the applied field. We establish in Appendix B the equations of motion for the electrons and fields, taking into account cylindrical symmetry in treating this three-dimensional problem. We solve simultaneously Poisson's equation (three dimensional), the system of conservation equation for the electrons and various ions, taking into account photoionization (creation of the initial charge densities), attachment of the electrons by oxygen to create O^- and O_2^- , photoionization of these negative ions by an auxiliary laser pulse (long laser pulse in the visible range), electron-ion and ion-ion recombinations, and finally elastic and ionizing collisions.

The calculations were applied to the model atmosphere, as well as to the laboratory testing cell. A typical result for the cell is shown in Figs. 3, where the field "on axis" (of the beam) is shown as a function of height, for various time increments.

In Fig. 3, successive plots of electric field versus height (in m) are shown, taken at 147 ns interval, following the creation of a "pencil" of photoionization with peak density in the center of $2 \times 10^{12} \text{ e}^-/\text{cm}^3$, and a Gaussian (vertical) distribution of 0.25 m width (FWHM). The radius of the pencil of electrons and positive ions created by fs UV photoionization is 400 μm . The applied electric field is assumed to be uniform and equal to 750 kV/m. Separation of charges result in a decrease of the field in the middle of the vertical distribution of charges. A very steep increase of the local field - and of charge density - occurs at the upper and lower boundaries of the ionized

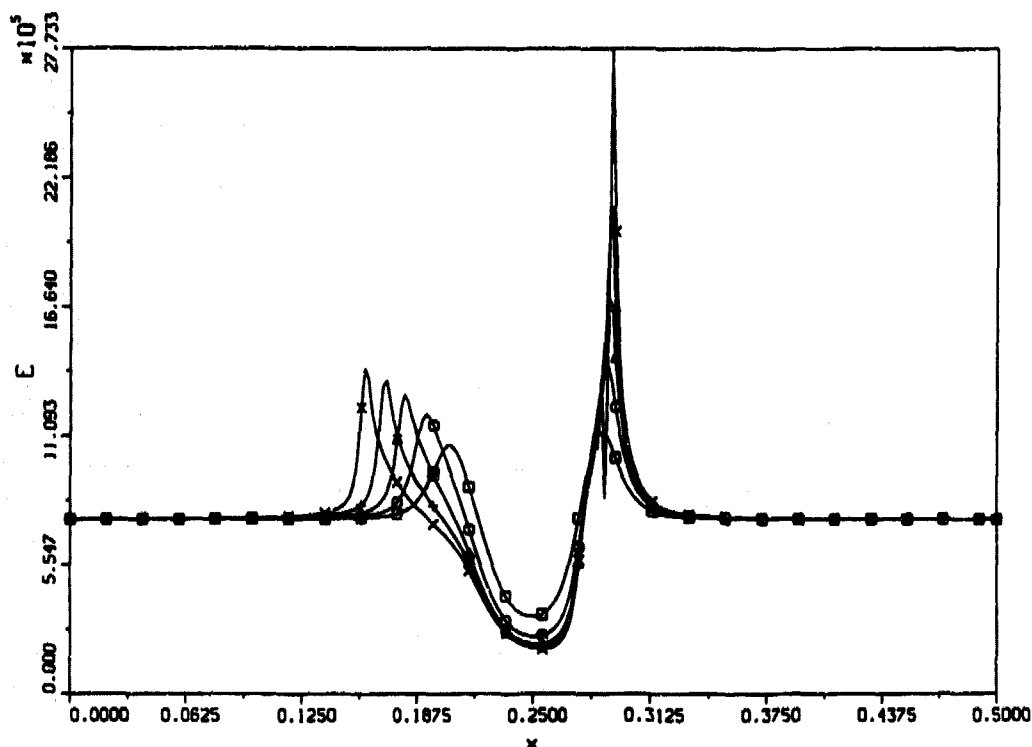


Figure 3:

Electric field in the laboratory cell versus height coordinate, for 5 successive time increments of 147 ns following fs photoionization of a cylindrical volume of $400 \mu\text{m}$ radius. The charge distribution is assumed to be uniform along the radial coordinate, and Gaussian along the axis of the cylinder, with a FWHM of 0.25 m. The applied field is uniform, equal to 750 kV/m.

volume, as shown in Fig. 3. The combined enhancement of the number of electrons and of the field leads to avalanche multiplication, initiating the discharge.

Numerous computer simulations show that the same qualitative picture emerges for the atmospheric situation.

6 Experimental work

In parallel to the theoretical work, laboratory tests have been performed, and a facility to study laser induced discharge in air has been constructed. The following tasks have been completed:

- Construction of a fs source of mJ pulses at 248 nm, consisting in a mode-locked dye laser at 744 nm, a 3 stage amplifier, a frequency tripler, and

an excimer laser amplifier.

- Construction of a 100 kV discharge chamber with *profiled electrodes*
- Measurement of the multiphoton ionization cross-sections of O_2 and N_2
- Observation of 100 kV discharge induced in dry air by 248 nm pulses

6.1 The oscillator

The oscillator is a dye laser (antiresonant ring) hybridly mode-locked, pumped by a mode-locked argon laser. The (100 %) pulse to pulse fluctuations of the dye laser oscillator makes the output of the chain an uncontrolled statistical event. The problem is illustrated by the oscilloscope recording of Fig. 4 showing a single sweep snapshot of the pulse train. It is only for the largest pulse, which occur with a probability of less than 10 %, that the amplified spontaneous emission can be suppressed in the amplifier chain. Considering that the high voltage discharge chamber cannot be fired at more than 1 shot/3 minutes, it is imperative to use an oscillator with a better duty cycle.

We have converted the dye oscillator into a Ti:sapphire mode-locked laser. The conversion is essential to have a reliable source of fs pulses for the laboratory analysis of the discharge. This laser provide self-mode locked pulses which reduced the number of optics inside the cavity and provides a stable uniform fs pulse train as shown in Fig. (5).

We expect 300 mW output beam from the laser consisting in a train of 200fs pulses at 744 nm with a repetition rate of 80 MHz. A tuning wedge will be inserted for wavelength selection and two SF14 prisms inside the cavity allows us to adjust the chirp of the pulses.

6.2 YAG laser Amplifier

These 25 nJ, 200 fs pulses will be amplified to 1 mJ by a amplifier (LDS751 as gain medium) pumped at 8 Hz by a frequency doubled Nd:YAG [11]. Initially designed with three stages, the amplifier has been recently upgraded with a fourth (last) stage using a "Bethune cell" to provide uniform pumping to the source pulse. The four stage amplifier provided 10^7 times amplification for the input pulses. The amplifier is shown in Fig. 6.

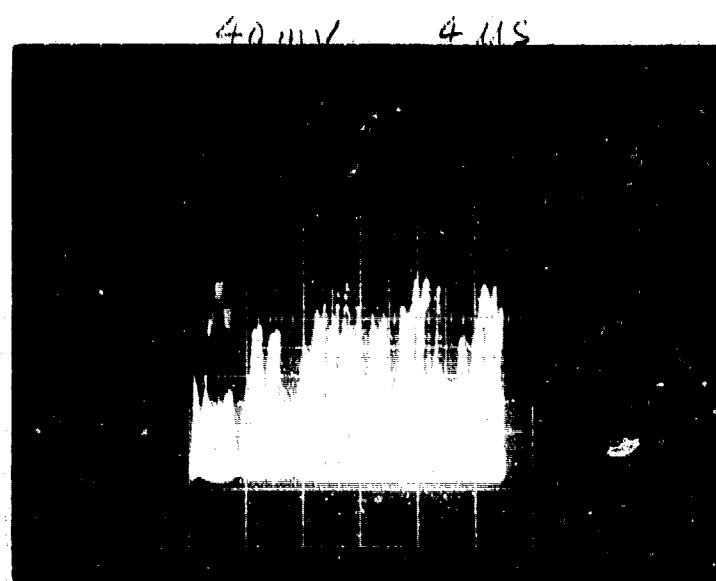
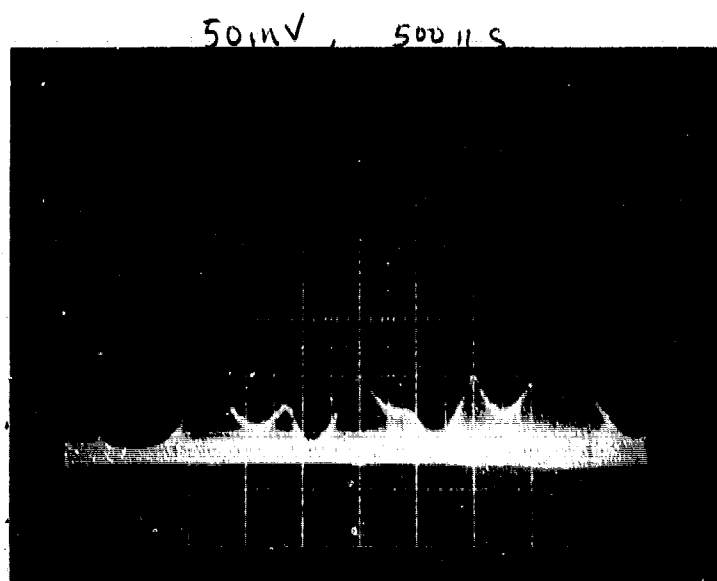


Figure 1: Oscilloscope trace (left: 500 ns/division, right: 4 μ s/division, single sweep) of the pulse train from the oscillator at 711 nm

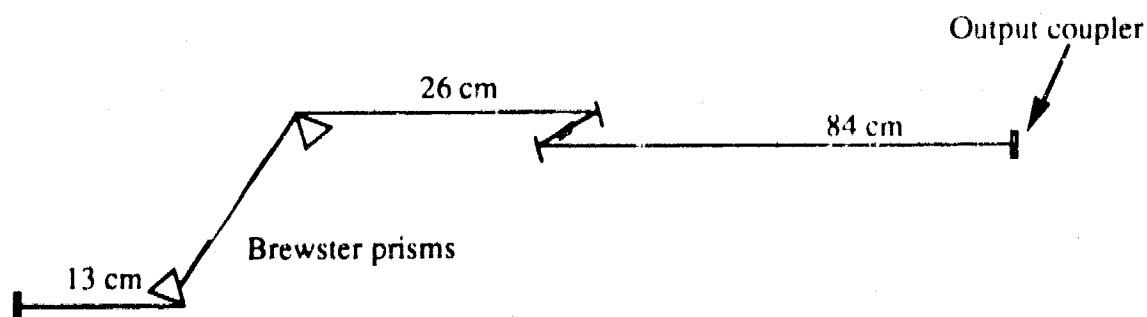


Figure 5: Self-mode locking Ti:sapphire laser.

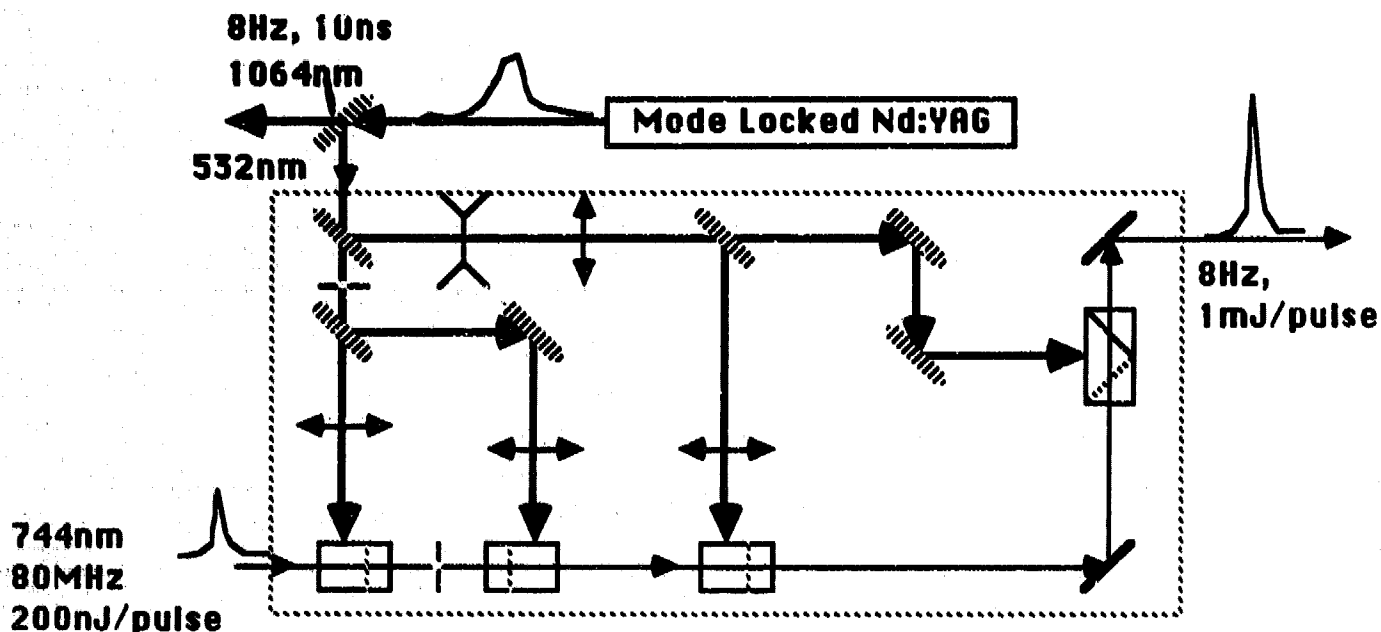


Figure 6: 8Hz YAG second harmonic pumped fs pulse amplifier

As usual, eliminating ASE and timing control between the pump and seeding pulses will be an important issue for the amplifier. Improved quality of the seeding pulse train, spatial filter inside the amplifier and the fine electronics time control should enhance the performance of the amplifier.

6.3 Frequency tripling assembly

The amplified pulses are focused into a 1 mm thickness KH_2PO_4 (KDP) to generate second harmonic and subsequently a 3 mm thickness KDP for the third harmonic generation. The setup is presented in Fig. 7.

Frequency tripling from 744 nm to 248 nm is performed with a sequence of two KDP crystals, cut for type I second harmonic generation (of 744 nm) and sum frequency (372 nm + 744 nm), respectively. A "dichroic" half wave plate (half wave at 372 nm, "zero wave" at 744 nm) is used between the crystals, with the purpose to rotate by 90° the polarization at 372 nm, leaving the polarization at 744 nm unchanged. Initially, the crystal and wave plate were all mounted on separate mount, resulting in a relatively poor conversion efficiency, because of the large spacing between crystals.

We are presently recalculating the Raleigh range and reconstructing the

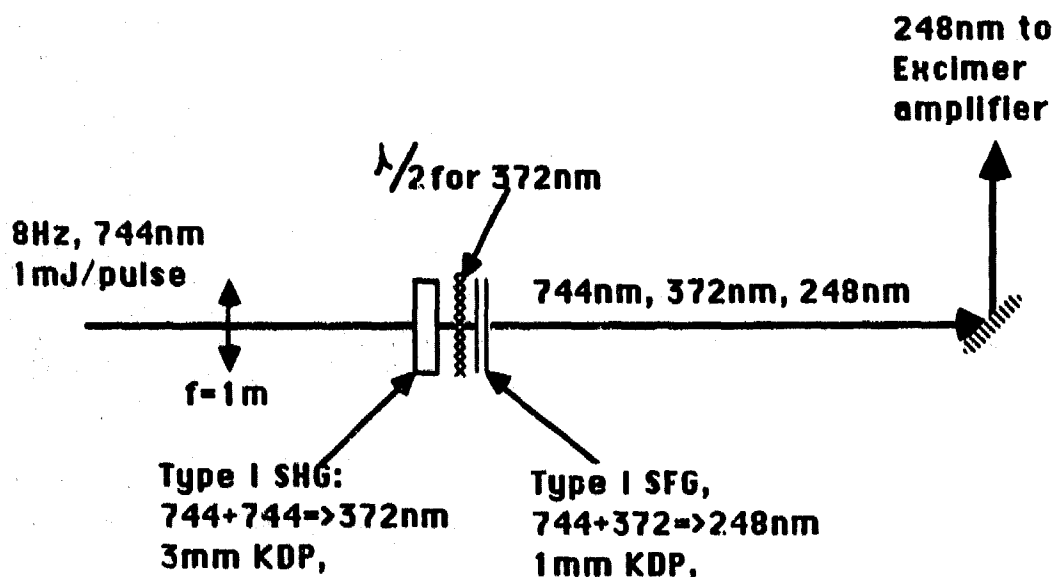


Figure 7: Setup for frequency tripling.

frequency tripling setup. The two nonlinear crystals and the half wave plate are assembled on a single mount and the distance from the front face of the first crystal to the rear face of the second crystal is minimized. The assembly ensures the two crystals are inside the focal region of the lens, to provide most efficient frequency conversion. The expected overall efficiency for third harmonic generation is about 1%.

6.4 KrF laser UV (248nm) pulse amplifier

The 248 nm pulses are amplified by an Excimer (KrF) laser (Questek) from 0.01 mJ/pulse to about 1 mJ/pulse. The KrF laser is modified into an amplifier. As shown in Fig. 8, the end mirror is replaced by an external cavity high reflector for double pass amplification.

The output pulses are focused into a spatial filter to filter out the ASE background.

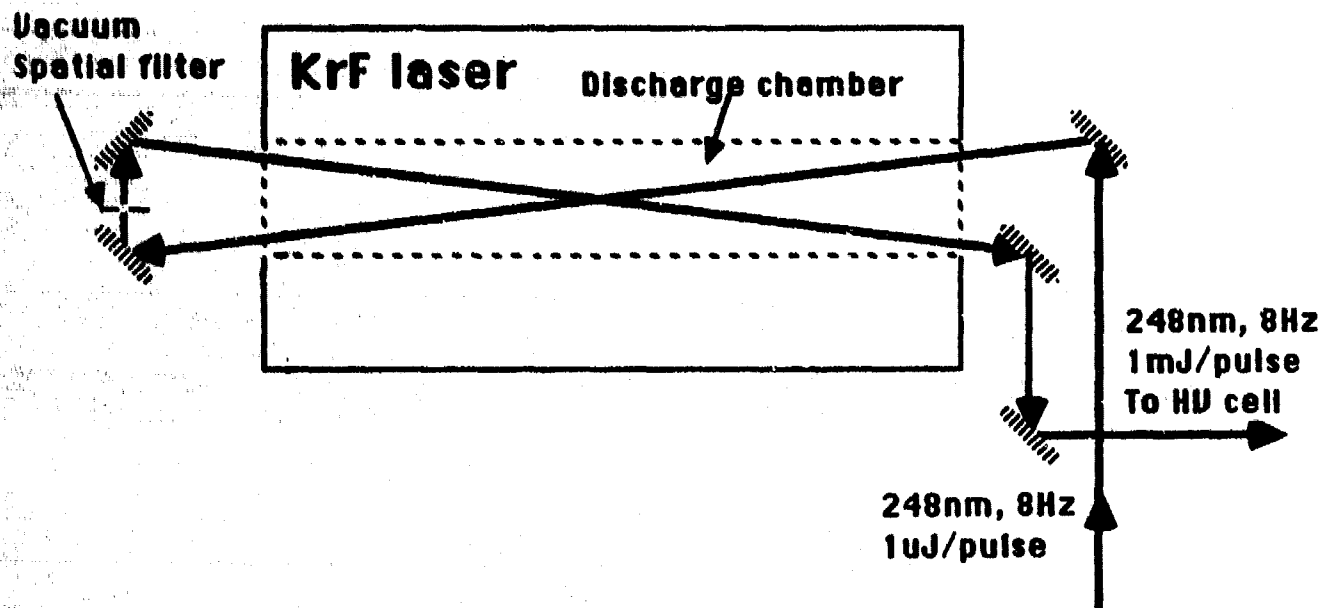


Figure 8: KrF UV fs pulse amplifier

6.5 Synchronizer

Because of the short life time (≈ 200 to 300 ps) of the amplifying dye (LDS751) and the thermal instability of the second harmonic crystal of the YAG laser, timing control of the laser-amplifier-amplifier system becomes very critical. A delay controlling electronic circuit has been designed and tested and proved to be helpful adjusting the timing with a jitter of less than 1 ns. The main "clock" is provided by the mode-locker of the argon laser at 40 MHz. That signal is divided down to 8 Hz by a digital divider. Each pulse from that divider is split, amplified and appropriately delayed to provide

- trigger for the flashlamps of the pump laser for the amplifier
- trigger for the Q-switch of the pump laser (jitter $\ll 1$ ns)
- trigger for the HV of the excimer laser
- trigger for the excimer discharge (jitter $\ll 1$ ns)
- trigger for the High voltage pulser

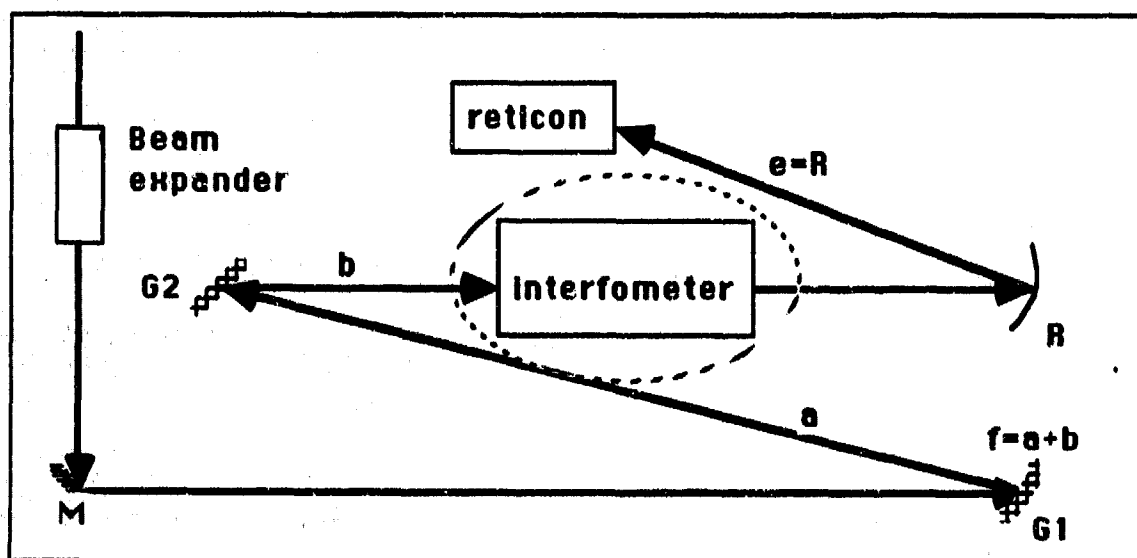


Figure 9: Experimental set-up for pulse duration and chirp measurement without nonlinear process

With the oscillator being modified into a self-mode locked Ti:sapphire laser, the electronics to synchronize the triggering setup has been modified. A photo diode detects signal from the source laser and sends it to a frequency divider. A divider has been constructed which reduces the frequency from 80 MHz to 8 Hz and provides proper delays to each of the triggering signals.

6.6 Pulse measurement without nonlinear process

Pulses at 248 nm can not be measured with conventional autocorrelator since no second harmonic is available at this wavelength. A linear single shot measurement of fs and ps pulses without nonlinear process has been developed. The setup provides us a tool for measuring the 8 Hz amplified pulses. The basic idea is presented in Fig. 9. Other methods using correlation requires a second harmonic crystal. For 248 nm this kind of crystal does not exist, this a new diagnostic method with all linear process is necessary. With this setup, we are able to determine the duration and the sign and amount of chirp of pulses.

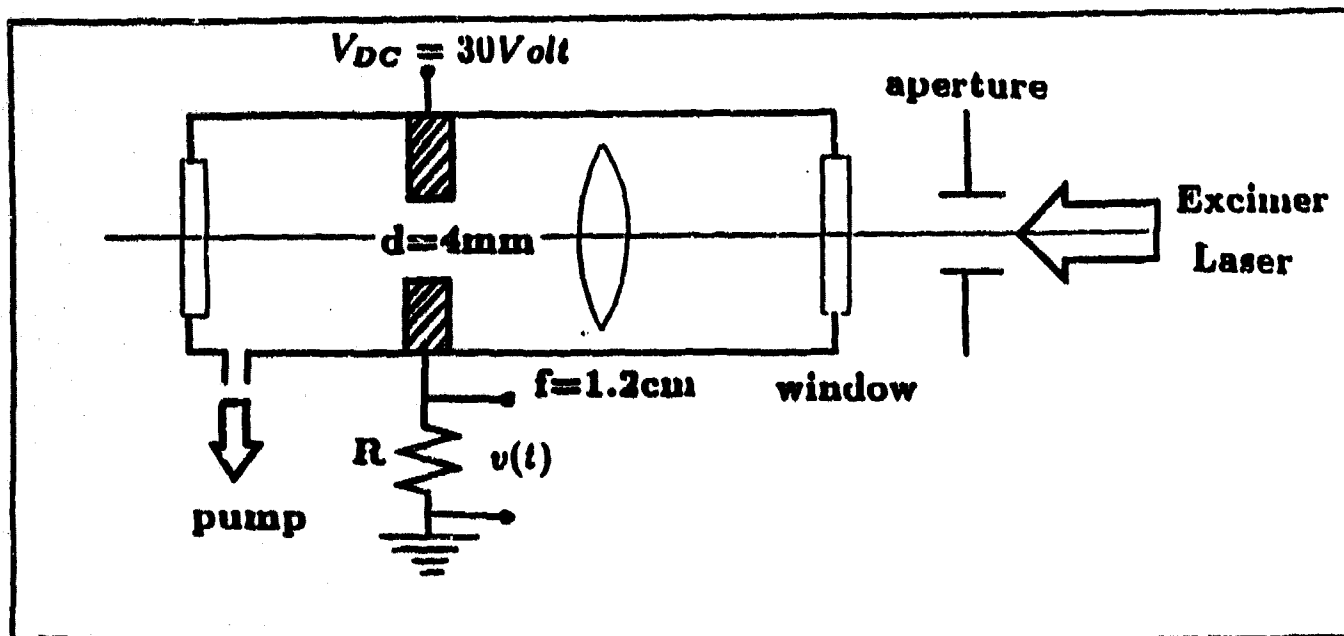


Figure 10: Experimental set-up for three and four-photon ionization cross-sections of O_2 and N_2 measurement.

6.7 Ionization cross sections

An experimental determination of the multiphoton ionization coefficients is made by collecting and measuring the photoelectrons in the set up of Fig. 10.

The mean free path of the electrons in the low pressure cell ($< 5 \times 10^{-4}$ torr) is much larger than the distance between the electrodes (4 mm). Therefore, the time integral of the current is a direct measure of the number of photoelectrons. At that low pressure however, the number of neutral molecules available for ionization soon saturates. Indeed, the number density of neutral molecules N_A decreases at the same rate at which the electron density N_e decreases:

$$\frac{dN_A}{dt} = -\frac{dN_e}{dt} = -\sigma^{(n)} I^n N_A, \quad (1)$$

where n denotes the order of ionization.

Our measurement shows that the three photon ionization for O_2 at 4×10^{-4} torr is $\sigma^{(3)} = 1.28 \times 10^{-23} J^{-3} s^2 cm^6$ which is sufficient to generate an electron density of $1.8 \times 10^{12} e^-/cm^3$ in air (at atmospheric pressure) with a 200 fs pulse at 248 nm having an energy density of $1 mJ/cm^2$. For N_2 at

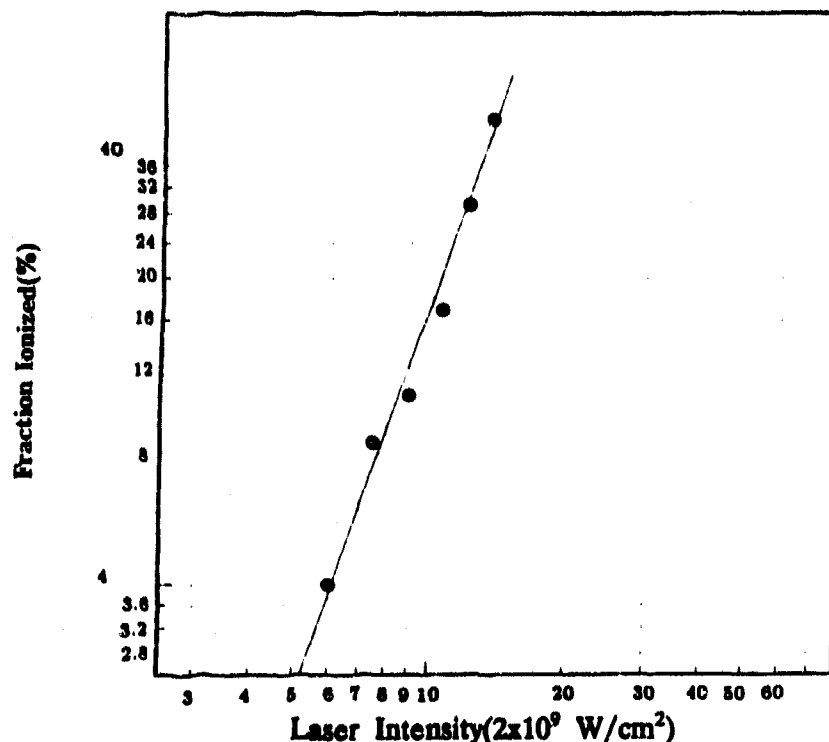


Figure 11: Measurement of three photon ionization cross-section of O_2 .

6×10^{-4} torr, we obtain four photon ionization $\sigma^{(4)} = 4 \times 10^{-34} \text{ J}^{-4} \text{ s}^3 \text{ cm}^8$ which is sufficient to generate an electron density of $1.0 \times 10^{12} \text{ e}^-/\text{cm}^3$ in the same condition as for O_2 . The results are presented in Fig. 11 and Fig. 12.

We use the measured σ 's to calculate the multiphoton attenuation coefficients β and γ used in Appendix A. We have $n\hbar\omega\sigma^{(n)}N_A I^{(n)} = \beta^{(n)} I^n$, i.e. $\beta^{(n)} = n\hbar\omega\sigma^{(n)}N_A$, with $\hbar\omega$ being the laser photon energy. We get $\beta = 1.6 \times 10^{-22} \text{ cm}^3/\text{W}^2$ for oxygen and $\gamma = \beta^{(4)} = 2.4 \times 10^{-32} \text{ cm}^5/\text{W}^3$ for nitrogen at atmospheric pressure.

6.8 High Voltage Cell

The high voltage chamber shown in Fig. 13. was fabricated by Tetra Corp to simulate the air environment. It has been tested in their company as well as in UNM. The system can be tested with an electronics triggering signal to have the current and voltage monitored during the discharge. The gating signal for applying HV onto the cell is synchronized with the seeding pulses through the control box. The detailed operation and characteristics are listed in a note delivered with the cell.

The test cell provides a nearly uniform electric field of 30 KV/m to 300

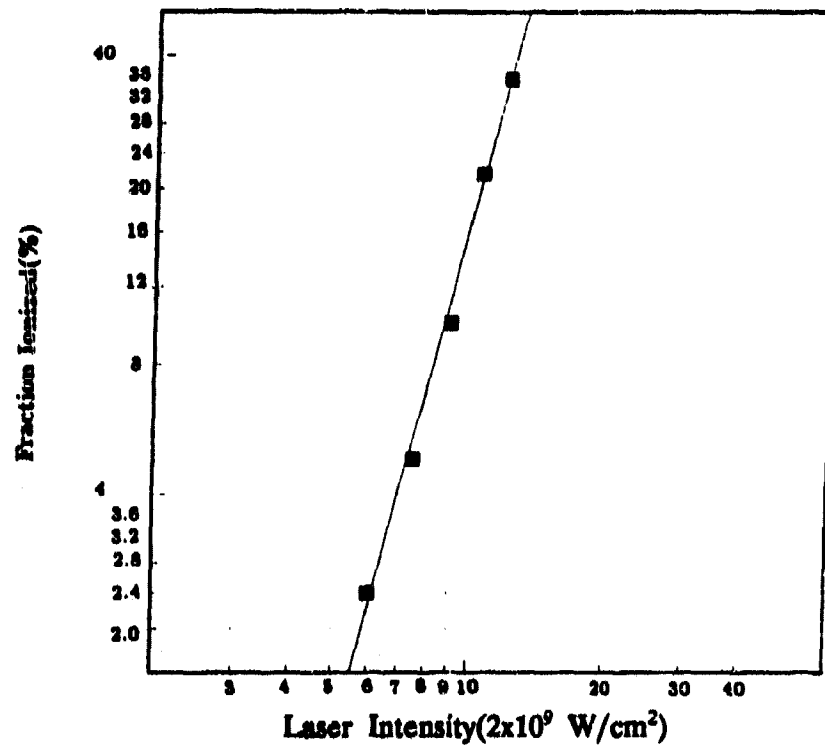


Figure 12: Measurement of four-photon ionization cross-section of N_2 .

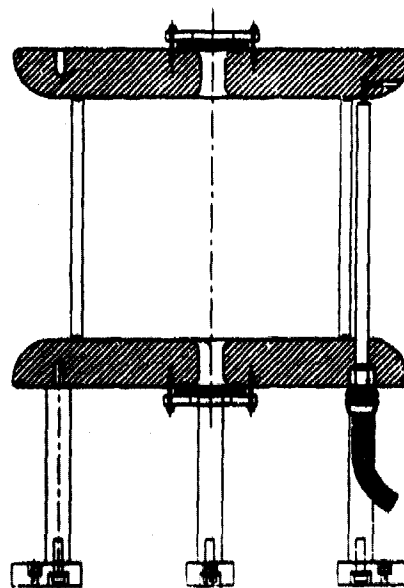


Figure 13: High voltage chamber for lightning simulation.

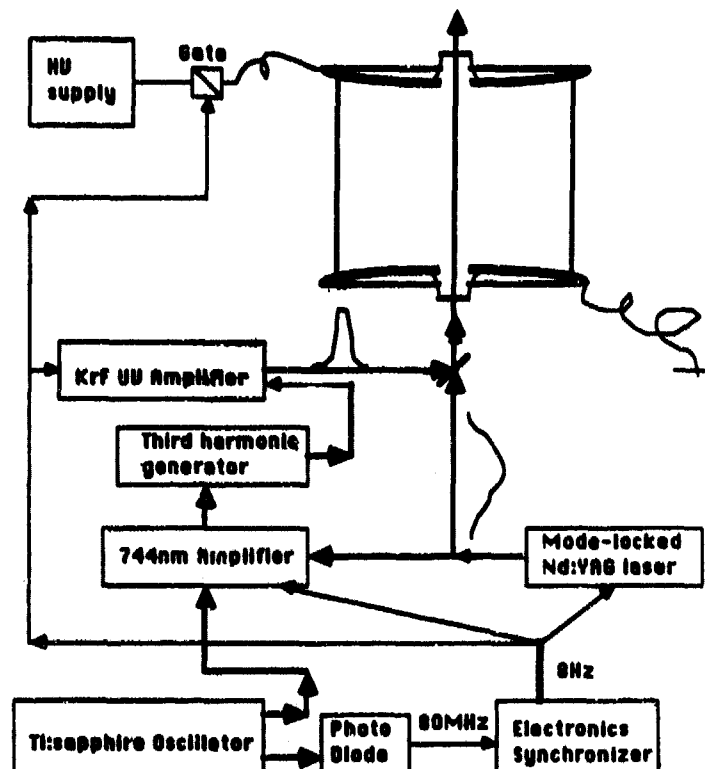


Figure 14: A complete setup for discharge of lightning experiment in the laboratory HV cell.

KV/m on the chamber within tens of microseconds. It consists of a chamber with profiled electrodes of 8.5 inch diameter spaced at 26 cm contained in a Lucite cylindrical housing. There is a two inch diameter hole at the center of each electrode sealed by a two inch diameter window made of MgF_2 . When the highest voltage is applied, the field is about 1/10 of the self breakdown field in air. The windows are recessed in a low field region to minimize the impact of a multiphoton photoelectric effect from the window surface.

6.9 Inducing 100 kV discharge in air

We trigger routinely a 100 kV discharge in air, N_2 and O_2 with 248 nm pulses from an excimer (KrF) laser. The complete setup for the lightning discharge is shown in Fig. 14 and a photograph of the discharge is reproduced in Fig. 15.

The discharge was induced with ns pulses of only 1 GW peak power, focused with a 60 cm focal distance lens between the electrodes of the discharge chamber. The discharge could readily be triggered at a pressure of 1/8 of an atmosphere, even though the peak intensity is two orders of magnitude below

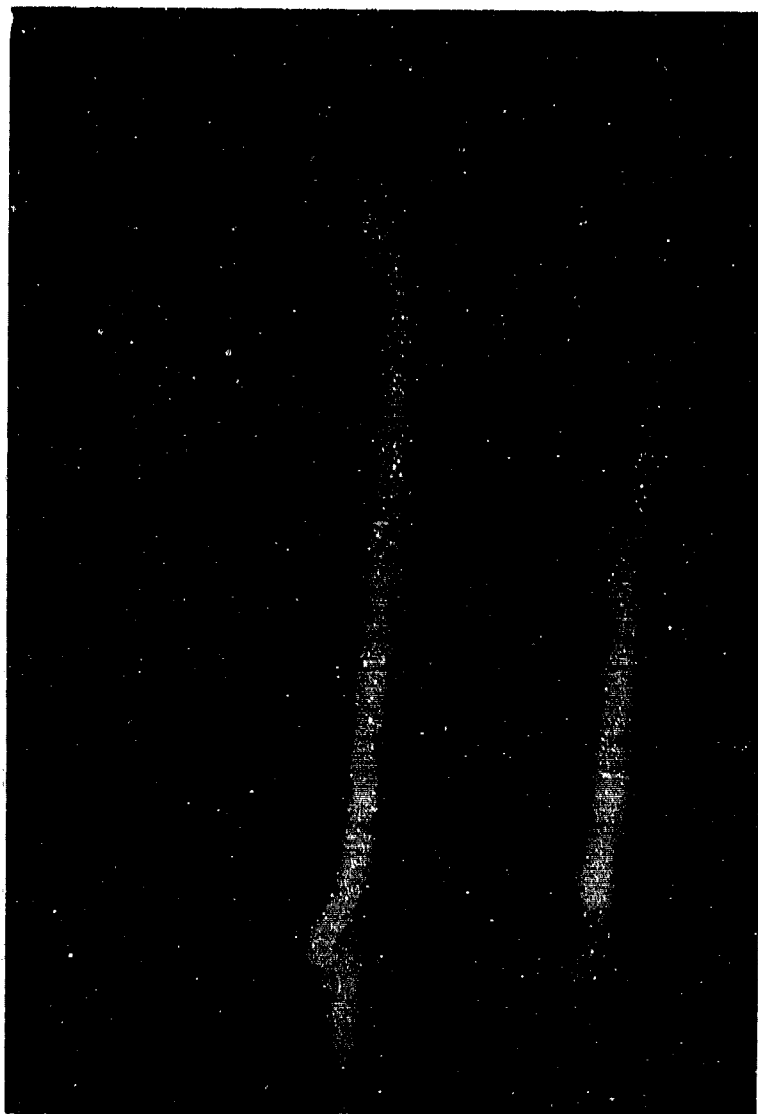


Figure 15: Electrical discharge in the laboratory cell ($1/7$ atmosphere) induced by a ns pulse of the excimer laser (peak power $1\text{GW}/\text{cm}^2$). The discharges follow the path of the beam, except that it bends towards a normal to the profiled electrodes at the two extremities.

that expected from the amplified fs pulses. This result confirms the exceptionally large multiphoton ionization cross-sections of nitrogen and oxygen, which we measured independently in a low pressure cell (see next section).

The discharge is *guided* by the light, as seen in the photograph. This result is significant, because the *preferential path for the discharge is not along the beam*. Indeed, in contrast to the experiment by the group in Japan [5], where the discharge is triggered between two needle shaped electrodes (hence there is a local field enhancement present *prior to the creation of the laser induced plasma*), our electrodes are profiled for uniform field. The holes leaving passage to the beam are profiled also. The field is *minimum* on axis, and the discharge observed at lower pressure, without laser triggering, never follow the axis of the cell, but is along the side wall of the chamber. Because the discharge should ultimately make contact at normal incidence with the electrodes, the two extremities of the discharge are bent towards the normal to the profiled hole in the electrodes.

7 Conclusion

We have demonstrated theoretically the feasibility to trigger lightning with fs pulses at 248 nm. Our measurements of photoionization of O_2 and N_2 at that wavelength show a very large cross-section for a three and four photon process. We have demonstrated that, at a reduced pressure of 1/7 atmosphere, even the peak power of a ns pulse is sufficient to channel a discharge and trigger lightning. A complete facility has been built to test the triggering of lightning with fs UV pulses in a reduced scale. Funds are being sought to operate this facility and proceed with a final experimental demonstration of triggering of lightning at atmospheric pressure, using fs UV pulses.

References

- [1] H. J. Christian, V. Mazur, B. D. Fisher, L. H. Ruhnke, K. Crouch and R. P. Perala. *The Atlas/Centaur Lightning Strike Incident*. J. of Geophysical Research, **94**, 169-177, 1989.
- [2] S. A. Changnon. *Temporal and Spatial Relations between Hail and Lightning*, J. of Appl. Meteorology. **31**, 587-604, 1992.
- [3] R. P. Fieux, C. H. Gary, B. P. Huzler, A. R. Eybert-Berard, P. L. Huber, A. C. Meesters, P. H. Perroud, J. H. Hamelin and J. M. Person. *Research on artificially triggered lightning in France*. IEEE Trans. Power Appar. Syst., **97**, 725-733, 1978.
- [4] P. Laroche, A. Eybert-Berard and L. Barret. *Triggered lightning flash characterization*. Tenth International Aerospace and Ground Conference on Lightning and Static Electricity (ICOLSE), Paris. pp.231-239, Les Editions de Physique, Les Ulis, France, 1985.
- [5] K. Nakamura and C. Yamanaka. Long laser-induced discharge in atmospheric air. In *Proc. CLEO*, Optical Society of America, 1992.
- [6] Xin Miao Zhao, Chao Yung Yeh, Jean-Claude Diels, and Cai Yi Wang. Ultrashort pulse propagation for triggering of lightning. In R. C. Sze and F. J. Duarte, editors, *Proceedings of the int. conf. on Laser's 91*. SPIE, SPS press, McLean, Virginia. San Diego, CA, December 1991.
- [7] Xin Miao Zhao, Chao Yung Yeh, Jean-Claude Diels, and Cai Yi Wang. Ultrashort pulse propagation for triggering of lightning. Conf. on Lasers and Electro-Optics, 1992. Anaheim, Ca.
- [8] S. Soula and S. Chauzy. The detection of the electric field vertical distribution underneath thundercloud - principle and applications -. pages 61-1 - 61-14. NASA Conference Publication 3106. Cocoa Beach, Florida, 1991.
- [9] Xin Miao Zhao, Chao Yung Yeh, Jean-Claude Diels, and Cai Yi Wang. Simulation on femtosecond pulse triggering lightning. In *Proc. of OSA Annual Meeting*. Optical Society of America, 1992. Albuquerque, NM.

- [10] Xin Miao Zhao, Chao Yung Yeh, Jean-Claude Diels, and Cai Yi Wang. A femtosecond lightning rod. In A. Migus, editor, *Picosecond Phenomena VIII*, page , Springer-Verlag, Berlin, 1992.
- [11] H. Vanherzeele, H. J. Mackey, and J. C. Diels, *Spatial and Temporal Properties of a Tunable Picosecond Dye-laser Oscillator-amplifier System*, Appl. Opt. B **23**, 2056-2061 (1984).

APPENDICES

A Pulse propagation/compression

The fs pulse centered at $\omega = \omega_t$ can be described by the complex envelope $\mathcal{E}(z, t)$ of the electric field $E(z, t)$:

$$E(z, t) = \frac{1}{2} \mathcal{E}(z, t) e^{i(\omega_t t - kz)} \quad (2)$$

If the nonlinear properties of air are neglected, the evolution of the pulse envelope with distance can be most easily calculated in the frequency domain:

$$\tilde{\mathcal{E}}(z + \Delta z, \omega) = \tilde{\mathcal{E}}(z, \omega) e^{-ik(\omega - \omega_t)z} \quad (3)$$

where $\tilde{\mathcal{E}}(z, \omega)$ is the Fourier transform of the envelope defined in Eq. (2). Expanding the wave vector k in a Taylor series around ω_t , and neglecting terms of order higher than 2, we find for the evolution of the field, in the retarded frame of reference:

$$\tilde{\mathcal{E}}(z + \Delta z, \omega) = \tilde{\mathcal{E}}(z, \omega) e^{-i\frac{k''}{2}(\omega - \omega_t)^2 \Delta z} \quad (4)$$

where $k'' = |\frac{d^2 k}{d\omega^2}|_{\omega_t} = 0.96 \cdot 10^{-28} \text{ s}^2/\text{m}$ for air. Considering 3 photon ionization to be the dominant loss mechanism:

$$\frac{dI}{dz} = -\beta I^3. \quad (5)$$

The above equation is easily integrated for a slice of air Δz :

$$\frac{1}{I^2(z + \Delta z)} = \frac{1}{I^2(z)} + 2\beta \Delta z. \quad (6)$$

Our measurements of the photoionization cross-section for N_2 indicate that the four photon process contributes significantly to the ionization and the pulse depletion. The propagation equation including 3 and 4 photon ionization is:

$$\frac{dI}{dz} = -\beta I^3 - \gamma I^4 \quad (7)$$

The propagation problem is solved numerically by applying successively the linear propagation Eq. (4) and the nonlinear absorption Eq. (6) to slices of air Δz . A fast Fourier transform is used to switch between time and frequency domains. As initial condition we take a pulse with a linear downchirp, which is focused by a lens.

B Evolution towards a streamer

We approximate the results of the preceding section by a cylinder of radius r containing a Gaussian distribution of electrons $N_e(z)$ and ions $N_i(z)$. Under influence of the external field, the electrons and ions will separate. However since the electrons are much lighter than the ions, we can assume that the electrons have been accelerated to a steady state velocity before any motion of the ions has even taken place. We establish in Appendix B the equations of motion for the electrons and fields, taking into account cylindrical symmetry in treating this three-dimensional problem.

The equation of motion of the electrons can thus be simplified:

$$m_e \frac{dV_e}{dt} = eE - m_e \nu V_e \approx 0 \quad (8)$$

$$V_e = -\left(\frac{e}{m_e \nu}\right)E = -\mu_e E \quad (9)$$

where μ_e is the electron mobility. We can substitute this expression (9) for the electron velocity in the conservation equation:

$$\frac{\partial N_e}{\partial t} + \frac{\partial}{\partial z}(V_e N_e) = 0, \quad (10)$$

to obtain:

$$\frac{\partial N_e}{\partial t} - \frac{\partial}{\partial z}(\mu_e E N_e) = 0. \quad (11)$$

Poisson's equation in one dimension:

$$\frac{\partial E}{\partial z} = \frac{e}{\epsilon_0}(N_i - N_e), \quad (12)$$

merely states that an internal field will appear as the charges separate, internal field which will cancel the effect of the applied field. In a one dimensional approximation, the presence of the charges only serves to neutralize the applied field. Rather than to treat rigorously a three dimensional problem, we can solve substitute for Eq. (12) the field calculated for a cylindrical distribution of *net charges* $\rho(z) = N_i(z) - N_e(z, t)$. Rather than solve Poisson's equation, this field is more easily derived from the integration of Coulomb

law applied to charged disks of thickness Δz and radius r :

$$E(z) = -\frac{1}{2} \left[\int_{-\infty}^0 \rho(z' + z) \left(-1 - \frac{z'}{\sqrt{z'^2 + r^2}} \right) dz' + \int_0^{\ell-z} \rho(z' + z) \left(1 - \frac{z'}{\sqrt{z'^2 + r^2}} \right) dz' \right] + E_{ext} \quad (13)$$

where ℓ is the height of the cylinder of charges, and r its radius. The time-space (z) evolution of the electric field is found by simultaneous integration of Eqs. (11) and (13), with as initial and boundary conditions:

$$\begin{aligned} N_e(z=0) &= 0 \\ E(t=0) &= E_{ext} \\ N_e(t=0) &= f(z) = N_i(z) \end{aligned} \quad (14)$$

The parameters are as follow.

$\mu_e = e/m_e \nu$ is the electron mobility. For $L_0 = 100$ m, $N_0 = 5.0 \times 10^{18} \text{ m}^{-3}$, and $\mu_e = 0.20 \text{ m}^2/\text{Vs}$, the units $t_0 = 5.5 \times 10^{-11} \text{ s}$ and $E_0 = 9.1 \times 10^{12} \text{ V/m}$. The average collision period $1/\nu$ with respect to the above μ_e is $1.1 \times 10^{-12} \text{ s}$. The enhancement typically occurs within several orders of magnitude of t_0 , the change of V_e is negligible, so that we can approximate $E = -V_e$. In the following numerical computation, we use the external electric field $E_{ext} = 500 \text{ kV/m}$, and the beam size $r = 1.0 \times 10^{-2} \text{ m}$, i.e., $E_{ext} = 5.5 \times 10^{-8}$ and $r = 1.0 \times 10^{-4}$ in the normalized unitless unit we use. For the laboratory experiment in the University of New Mexico, we use $L_0 = 0.5 \text{ m}$, $r = 2.0 \times 10^{-4} \text{ m}$, $E_{ext} = 175 \text{ kV/m}$ and N_0 and μ_e are same as before. Then $E_0 = 4.5 \times 10^{10} \text{ V/m}$ and t_0 is same as before. In our unit, $E_{ext} = 3.9 \times 10^{-6}$ and $r = 4.0 \times 10^{-4}$.

A computer program written with a flux corrected transport (FCT) algorithm is used to simulate the time evolution of electron density and electric field. The initial condition for electron density comes from the laser induced ionization, discussed in Appendix A. The setup time for the initial condition is $L_0/c = .33 \mu\text{s}$ for $L_0 = 100 \text{ m}$, where c is the light speed. We denote the initial condition symbolically as

$$N_e(z, t=0) = N_i(z) = f(z). \quad (15)$$

The boundary conditions for the equations are

$$N_e(z=0, t) = N_e(z=1, t) = 0, \quad (16)$$

and

$$E(z = 0, t) = E(z = 1, t) = E_{ext}, \quad (17)$$

where $z = 0$ and $z = 1$ are far from the region where electron and ion densities are not equal to zero.